LODZ UNIVERSITY OF TECHNOLOGY
FACULTY OF MECHANICAL ENGINEERING
DEPARTMENT OF DYNAMICS

inż. Mateusz Lazarek
177904

inż. Michał Niełaczny
177908

MASTER OF SCIENCE THESIS
Mechanical Engineering: Mechanical Engineering & Technology
Full-time studies

SYNCHRONIZATION OF SLOWLY ROTATING PENDULUMS

supervisor:
prof. dr hab. inż. Tomasz Kapitaniak

INNOVATIVE ECONOMY
NATIONAL COHESION STRATEGY
FNP Foundation for Polish Science
EUROPEAN UNION
EUROPEAN REGIONAL DEVELOPMENT FUND

Contents

1 Introductions **4**
- 1.1 The aim of the thesis . . . 4
- 1.2 Theoretical background . . . 4

2 Model **8**
- 2.1 Mathematical model . . . 8
- 2.2 Actual model . . . 10

3 Parameters **12**

4 Electronic circuits **15**
- 4.1 Assumptions of the project . . . 15
- 4.2 Test circuit . . . 16
- 4.3 Final circuit . . . 17
- 4.4 Software . . . 19
- 4.5 PWM signal . . . 21
- 4.6 Reading signal frequency . . . 21
- 4.7 USART Interface . . . 22

5 First model's synchronizations **23**

6 Measurements and elaborated results **25**
- 6.1 Two pendulums . . . 25
  - 6.1.1 Two pendulums' completely synchronization . . . 25
  - 6.1.2 Two pendulums synchronization at 180° intervals . . . 27
- 6.2 Three pendulums . . . 28
  - 6.2.1 Three pendulums' completely synchronization . . . 28
  - 6.2.2 Three pendulums synchronization at 120° intervals . . . 29
- 6.3 Oscillation periods . . . 30

7 Conclusions **31**

List of denotations

c_φ – damping coefficient on motor's shaft,
d_y – damping coefficient in coefficient,
g – gravity acceleration,
$f_{clkI/O}$ - I/O Clock frequency.
I_w – mass moment of inertia of pendulum,
k_y –stiffness coefficient in coefficient,
l – length of pendulum,
m_w – mass of pendulum,
m_i – point mass at the end of pendulum,
M_0 – mass of beam with dc motors,
M_c – mass of whole system,
N - the prescaler divider (1, 8, 64, 256, or 1024),
N_i – forcing torque,
R – Rayleigh dissipation,
T – total kinetic energy,
v_i – linear velocity of point mass,
v_{wi} – linear velocity of center of mass of i-th pendulum,
V – potential energy,
φ_i – angular displacement of i-th pendulum,

Chapter 1

Introductions

1.1 The aim of the thesis

The aim of this thesis is to create research station to examine synchronization of three slowly rotating pendulum, which includes:

- Creation of a desired electronic circuit,
- Writing own programs for control of the system,
- Creation of mathematical model,
- Perform numerical analysis,
- Building actual model,
- Obtaining synchronization of pendulums:
  - Two pendulums – completely and faze at 180° intervals,
  - Three pendulums – completely and faze at 120° intervals,
- Comparing theoretical and actual results.

1.2 Theoretical background

According to a definition with pendulum we name the body fastened of above its center of heaviness which effects twitching in a vertical plane, under the influence of the force of gravitation. We distinguish two, usually applied in mechanics, types of pendulums:

- Physical
- Mathematical

A physical pendulum is a material body suspended on a horizontal axis, so as to it could rotate around it [1]. A mathematical pendulum, which is an idealized physical pendulum, is a material point combined by rigid, imponderable rod with a base by a rotary knot enabling fluctuations and rotations in a plane.

Word synchronization has a greek root origin (originally means "to share the common time"). Research work of synchronization phenomenon started in the 17th century and first reported discovery was made by Huygens in phase synchronization of weakly coupled pendulum clocks. Synchronization in coupled dynamical systems is associated with the emergence of collective coherent behavior between identical or similar subsystems.

Dynamic structures can be divided into chaotic or not chaotic systems. Chaotic system is the one which evolution depends on the initial conditions. This paper investigates system able to synchronize despite differences of initial conditions which determines it as not chaotic.

Mechanical systems, with rotating parts, are typical in engineering applications and subject of intensive studies. Problem of scientific interest, which among others occurs in those systems, is the phenomenon of synchronization of different rotating parts. Synchronization in coupled dynamical systems is associated with the emergence of collective coherent behavior between identical or similar subsystems. Different initial conditions are not much important. After a sufficiently long transient, the rotating parts move in the same way. Complete synchronization, or synchronization at permanent constant interval is established between their displacements. Synchronization occurs due to dependence of the periods of rotating elements motion and the displacement of the base on which these elements are mounted [2]. In 17th century Huygens reported his discovery of tendency of two pendulums (of the clocks) coupled through elastic structure (beam) to synchronize. It was the first observation, that has application in physics, of phenomenon of coupled harmonic oscillators. Kanunnikov and Lamper prove that accurate antiphase motion of pendulums with different masses cannot occur. Pogromsky created a controller which solves the synchronization problem. Pendulums reach required level of energy and move synchronously in opposite directions. [3]

This paper is experimental verification of theoretical background made by prof. dr hab. inż. Krzysztof Czołczyński. In his articles he investigates the to case of synchronizations: rotating pendulums in the horizontal plane, with non-gravity influence on their motion, and pendulums rotate in the vertical plane, with gravity influence on their motion [2]. His other attempt was to examine similar system consisting of n pendulums mounted on the movable beam. In this case the pendulums are excited by the external torques. Relation between the angular velocities of the pendulums and torque is linear [4].

Systems with N degrees of freedom, can be described by N generalized coordinates q_i, $i = 1, 2, ..., n$. Lagrange equations of the second kind have the following form:

$$T = \frac{d}{dt}(\frac{\delta T}{\delta \dot{q}_i}) - \frac{\delta T}{\delta q_i} + \frac{\delta R}{\delta \dot{q}_i} + \frac{\delta V}{\delta q_i} = Q_i \tag{1.1}$$

where T is kinetic energy, V potential energy, R Rayleigh's dissipation function and Q_i is generalized external force acting on system. Q_i is given by:

$$Q_i = \sum_l F_l \frac{\delta r_l}{\delta q_i} + \sum_l M_l \frac{\delta \omega_l}{\delta \dot{q}_i} \tag{1.2}$$

where F_l and M_l are vectors of external forces and moments respectively, r_l is position vector in relation to point of force F_l application and ω_l is angular velocity of the system in relation to point of moment M_l application. The products in the above formula are scalar products [5].

Take into consideration electronic circuits presented system is equipped with microcntroller application based on AVR processor. AVR circuit architecture has the 32 registers which are directly connected to the Arithmetic Logic Unit (ALU). That configuration allows two independent registers to be accessed in one single instruction executed in one clock cycle. As a result more code efficiency is reached - throughputs is up to ten times faster than conventional CISC microcontrollers.

The Atmel AVR processors are characterized by the following features. Circuit Memory is divided into sections: In-System Programmable Flash with Read-While-Write capabilities, EEPROM and SRAM. AVR circuit can be equipped with: Real Time Counter (RTC), Timer/Counters with compare modes and PWM, USARTs, 2-wire Serial Interface, ADC with optional differential input stage with programmable gain, programmable Watchdog Timer. his type of processors can be programed by SPI or JTAG interface [6].

Another main part of the system is one responsible for motor control - an H-bridge. The H-bridge is an electronic circuit which enables a voltage to be applied across motor's terminals in either direction. These circuits are often used in robotics and other applications to allow DC motors to run forwards and backwards. H-bridges are available as integrated circuits, or can be built from discrete components.The H-Bridge arrangement is generally used to reverse the polarity of the motor, but can also be used to 'brake' the motor, where the motor comes to a sudden stop, as the motor's terminals are shorted, or to let the motor 'free run' to a stop, as the motor is effectively disconnected from the circuit [7].

Chapter 2

Model

2.1 Mathematical model

A 2D system is considered, which is shown below, in Figure 2.1. The beam of mass M_0 can move only vertical direction. The beam is considered as a rigid body. The beam is connected to a stationary base by light spring with stiffness coefficients k_y and viscous damper with a damping coefficients d_y. The beam supports three rotating excited pendulums with exactly same length l and mass m_w. To the each pendulum is attached point mass m_i $(i = 1, 2, 3)$. The rotation of the $i - th$ pendulum is given by a variable φ_i and its motion is damped by the viscous friction described by damping coefficient c_φ. The forces of inertia, with which each pendulum acts on the beam, cause its motion in a horizontal direction (described by the coordinate x), and in a vertical direction (described by the coordinate y). The pendulums are excited by external torques N_i. We assumed that the system is in gravitational field (where constant $g = 9.81$ is the acceleration due to gravity), but no other external forces act. The gravitational field causes the unevenness of its rotation, i.e., the pendulum slows down when the center of its mass goes up and accelerates when the center of its mass goes down. [4]

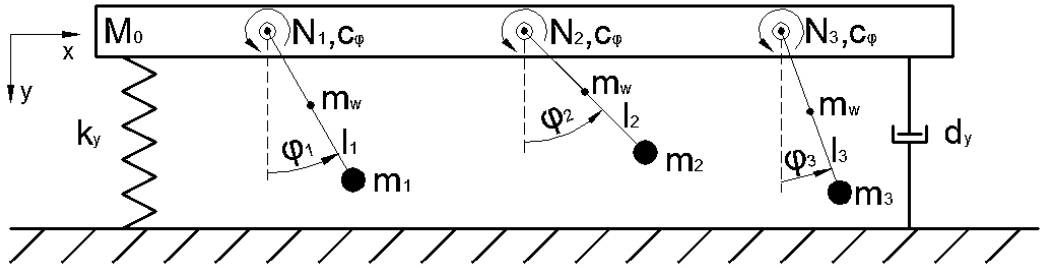

Fig. 2.1: Mathematical model of the system

Total kinetic energy T of the system is given by:

$$T = \frac{1}{2}M_0\dot{y}^2+\frac{1}{2}m_w(v_{w1}^2+v_{w2}^2+v_{w3}^2)+\frac{1}{2}m_1v_1^2+\frac{1}{2}m_2v_2^2+\frac{1}{2}m_3v_3^2+\frac{1}{2}I_w(\dot{\varphi}_1^2+\dot{\varphi}_2^2+\dot{\varphi}_3^2) \tag{2.1}$$

where:

$$I_w = \frac{1}{12}m_w l^2 \tag{2.2}$$

Potential energy V of the system is given by:

$$V = \frac{1}{2}k_y y^2 + M_c g y - \sum_{i=1}^{3}[(\frac{1}{2}m_w + m_i)lgcos\varphi_i] \tag{2.3}$$

where:

$$M_c = M_0 + 3m_w + m_1 + m_2 + m_3 \tag{2.4}$$

Rayleigh dissipation R is given by:

$$R = \frac{1}{2}d_y\dot{y}^2 + \frac{1}{2}c(\dot{\varphi}_1^2 + \dot{\varphi}_2^2 + \dot{\varphi}_3^2) \tag{2.5}$$

The system can be described by four equations written in a form of Euler-Lagrange equations:

$$\begin{cases} M_c\ddot{y} + d_y\dot{y} + k_y y + M_c g - \sum_{i=1}^{3}[(\frac{1}{2}m_w + m_i)l(\ddot{\varphi}_i sin\varphi_i + \dot{\varphi}_i^2 cos\varphi_i)] = 0 \\ (\frac{1}{3}m_w + m_1)l^2\ddot{\varphi}_1 - (\frac{1}{2}m_w + m_1)l\ddot{y}sin\varphi_1 + (\frac{1}{2}m_w + m_1)glsin\varphi_1 + c_\varphi\dot{\varphi}_1 = N_1 \\ (\frac{1}{3}m_w + m_2)l^2\ddot{\varphi}_2 - (\frac{1}{2}m_w + m_2)l\ddot{y}sin\varphi_2 + (\frac{1}{2}m_w + m_2)glsin\varphi_2 + c_\varphi\dot{\varphi}_2 = N_2 \\ (\frac{1}{3}m_w + m_3)l^2\ddot{\varphi}_3 - (\frac{1}{2}m_w + m_3)l\ddot{y}sin\varphi_3 + (\frac{1}{2}m_w + m_3)glsin\varphi_3 + c_\varphi\dot{\varphi}_3 = N_3 \end{cases}$$

2.2 Actual model

First actual model of the system is shown in Figure 2.2. The wooden beam is mounted by four sponges on the stationary wooden base. Sponges perform function both as springs and also as vicious dampers. The beam supports three direct-current motors with one pendulum attached to each. At the end of each pendulum is attached unbalance in form of screw with nut and several washers. Pendulums are drawn in Inventor and cut out in aluminum. A program to the cut out of pendulums is written in Edgcam for numerically controlled machine. Control system is located outside our stand.

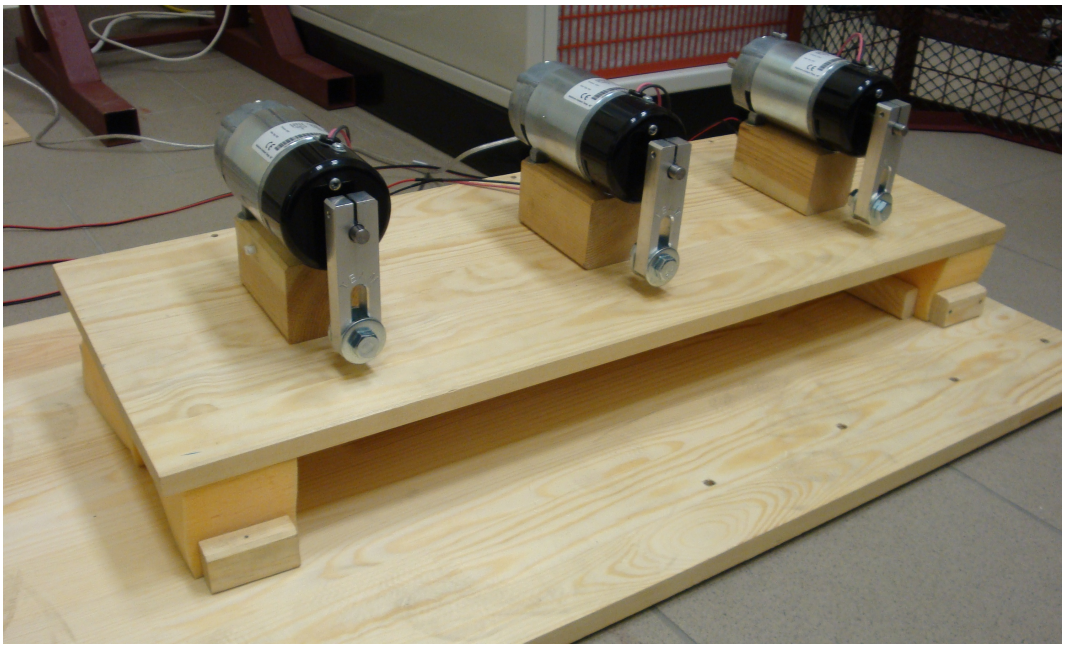

Fig. 2.2: First actual model of the system

The first actual model was good enough to obtain synchronization of pendulums. Instead, not sufficient. During the synchronization of pendulums, appears unwanted phenomenon. The system rotates round a transverse axis of beam. It means, that middle motor practically does not change a position, while both terminal, move alternate up and down. In fact, every motor have other referring plane. This model is not sufficient for the sake of too much degrees of freedom. By reason of this, results could not be clearly related to mathematical model.

To exclude this phenomenon, five beam's degree of freedom is removed. Only vertical displacement is leaved. It is obtained through the attaching of motors on a wooden beam which one can rotate round one of ribs. This one can be observed in Figure 2.3, which shows an ultimate model. At one end of the beam hinges were installed, which are connected with stationary base, made of a kitchen table-top, by wooden distance. At opposite rib, motors with pendulums and encoders are attached. In this model, sponges are also used as springs and vicious dampers. Control system is installed at the end of table-top, and interfaced is user-friendly. The whole is fixed to rails locating in a floor.

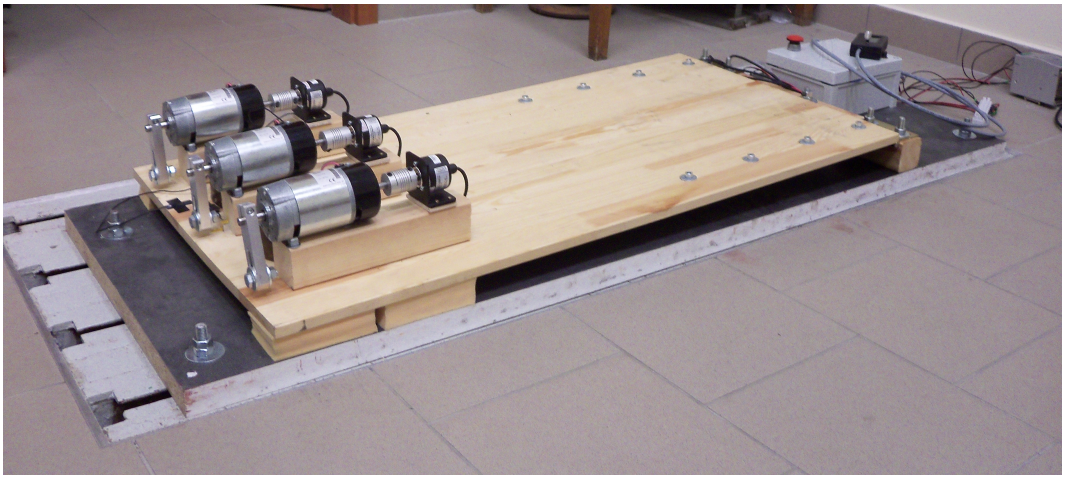

Fig. 2.3: Ultimate actual model of the system

Taking into consideration that beam is sufficiently long, and vibrations are small, order of magnitude of millimeters, it can be assumed that displacement of motors are lineal. Most important is the fact that all motors, in each time moment, have the common referring plane.

Chapter 3

Parameters

Indispensable for numerical analysis is knowledge of parameters, like damping and stiffness coefficients, of the system. Values of parameters are measured by ultimate actual model, and determined by mathematical model. Following, every values are compared and averaged.

Stiffness coefficient k_y was obtained, in experimental way. Four sponges are used to support beam with pendulums .It was measured by Micro-Epsilon distance laser detector. Detector was set up on stand above wooden beam near rib with motors. The beam was load by following weights. We measured increment of voltage by Kemot voltmeter and changed it into centimeters, definition - 4V for 5cm.

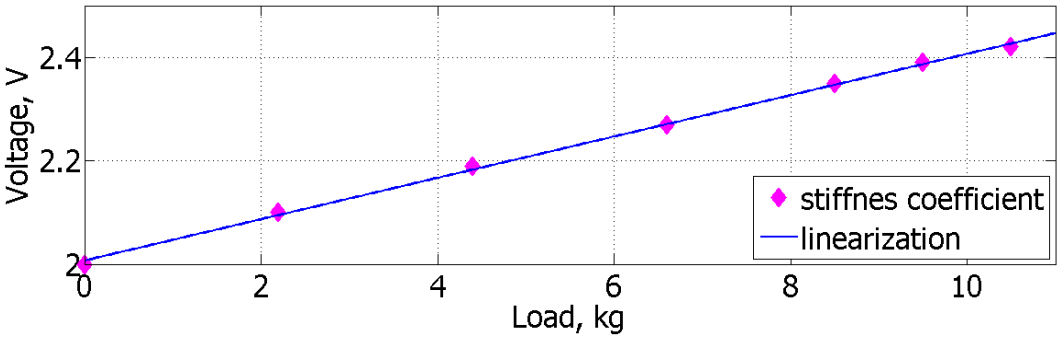

Fig. 3.1: Measurement of stiffness coefficient of sponges in vertical direction.

Coefficient k_y is a tangent of angle of slope of a curve, and it amounts $k_y = 3745N/m$.

Damping coefficient d_y is measured by KB10 sensor during free oscillations of the beam with pendulums. Three modes of vibration have been forced

and computer analyzed. KB10 sensor is connected to Veb RFT Messelektronik Otto Schön's amplifier. Following data is output to HP oscilloscope. Readouts from oscilloscope, by program BenchLink Scope, was loaded into Microsoft Excel.

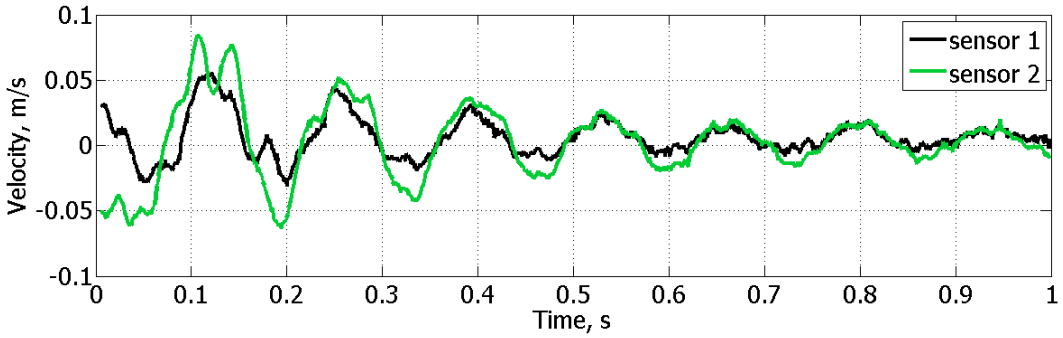

Fig. 3.2: Natural frequency forced in x direction

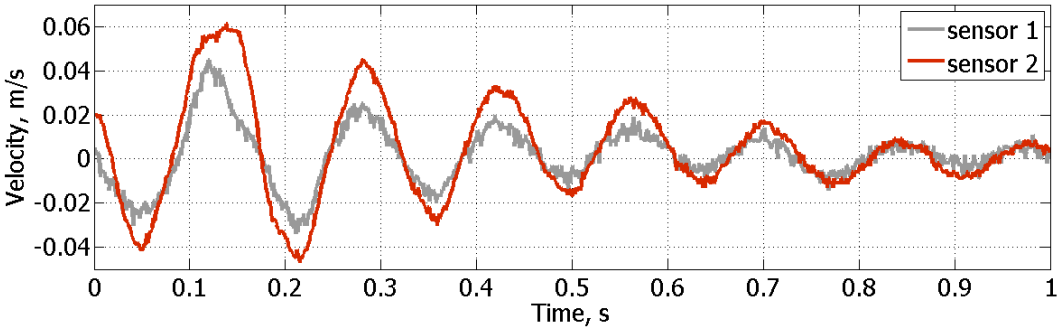

Fig. 3.3: Natural frequency forced in y direction

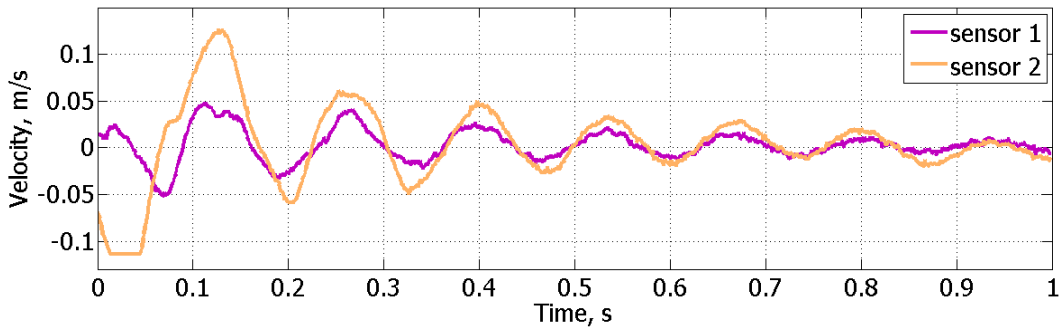

Fig. 3.4: Natural frequency forced around z direction

From plot, logarithmic decrement is calculated, using following formulas:

$$\Delta = ln(amp_1 - amp_2) = hT \tag{3.1}$$

Knowing logarithmic decrement and natural period from plots, damping coefficient can be calculated. Following, received dependences:

$$h = \frac{d_y}{2M_c} = \frac{ln(amp_1 - amp_2)}{T} \tag{3.2}$$

$$d_y = \frac{2M_c ln(amp_1 - amp_2)}{T} \tag{3.3}$$

Damping coefficient of sponges amounts $d_y = 7Ns/m$.

Below, in Table 3.1, are shown parameters used to numerical simulations.

Parameters	**Denotations**	**Value**	**Unit**
Mass of pendulum	m_w	0.1062	kg
Length of pendulum	l	0.075	m
Mass of beam	M_0	16.5	kg
Point mass at the end of pendulum	m_i	0.0792	kg
Damping coefficient	d_y	7	Ns/m
Motor damping coefficient	c_φ	7	Ns/m
Stiffness coefficient	k_y	20000	N/m
External tourqe	N_i	0.5 v 0.17	Nm

Tab. 3.1: Parameters

Chapter 4

Electronic circuits

4.1 Assumptions of the project

Assumptions of the presented project were clearly shown at the beginning of the work. Main functionality was the ability to have independent control of three DC motors. Work on tasks was fought simultaneously on two independent systems - test and final. Further work in the system allowed the development of the following options:

- Control of all the functions of the system which ware operated by the menu,
- Possibility to observe the action of the system on an 2x16 alphanumeric screen,
- Knowledge of the actual motors speed,
- Possibility to control system in two and three pendulums configurations,
- Independently setting motor speed by changing duty cycle of PWM signal,
- Independently setting actual motor speed.

4.2 Test circuit

Test circuit was developed for software testing. The main part is Atmel microprocessor - ATmega328p which provides most features of ATmega processors but it also has same boundaries [8]. As an integral part DC-DC voltage regulator based on popular 7805 regulator was constructed [9]. The VNH5019 Motor Driver Carrier made by Pololu company, was used as motor control unit [7] [10]. These systems along with the use of an oscilloscope allowed the development of the method of frequency measurement. Due to limited processor properties system can operate only with one motor. All procedures ware copied to the final circuit which is described in 4.3 section. Test circuit is shown in the Figure 4.1

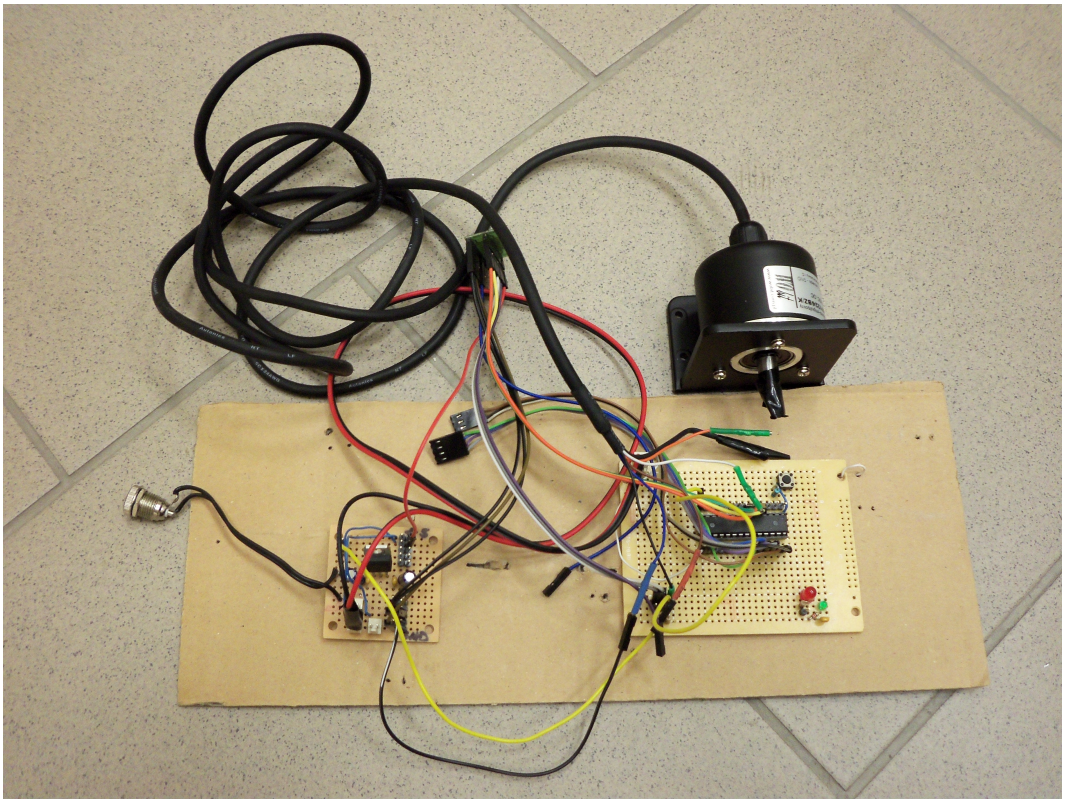

Fig. 4.1: Test circuit

4.3 Final circuit

The main change between test and final circuit was the usage of commercial platform based on Atmega2560 microprocessor. Due to erase all software made by manufacturer it is possible to have an access to full processor memory. Atmega2560 is a 8-bit AVR Microcontroller with 256KB of the Flash memory and it has 100-pin. The most important feature of this chip is that it is possessed with 4 Input Capture Channels of which two are used to reading motor speed [6]. More information of the measuring method is presented in 4.6 subsection.

Three encoders bought from the Wobit company are used. These sensors are characterized by high resolution - 2500 impulses per revolution. Each of them has two phase shift high resolution channels and one named 0 which indicate one impulse per revolution [11]. Chosen microcontroller has only a few inputs that are able to receive such signals. Such system configuration leads to the use of the choosing input signal system. Usage of 4051 multipleksers gave such opportunity [12]. In order to gathering data from encoders dedicated circuit containing another Atmega2560 was constructed. Ideological schematic of the system is presented in Figure 4.5. Actual execution is shown in Figures: 4.2 4.3 4.4

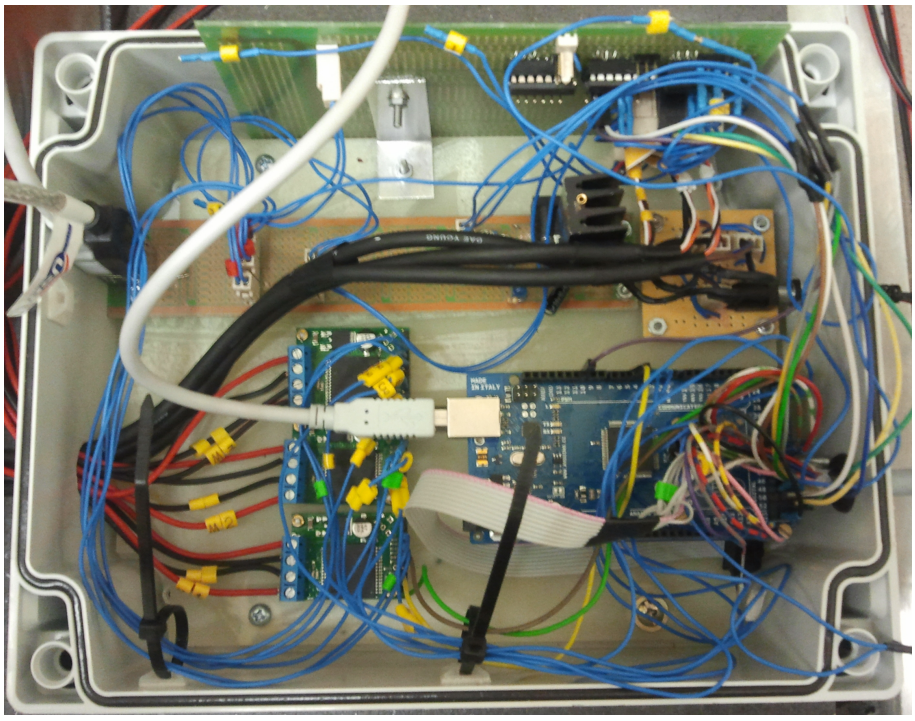

Fig. 4.2: Final circuit electronic - inside box view

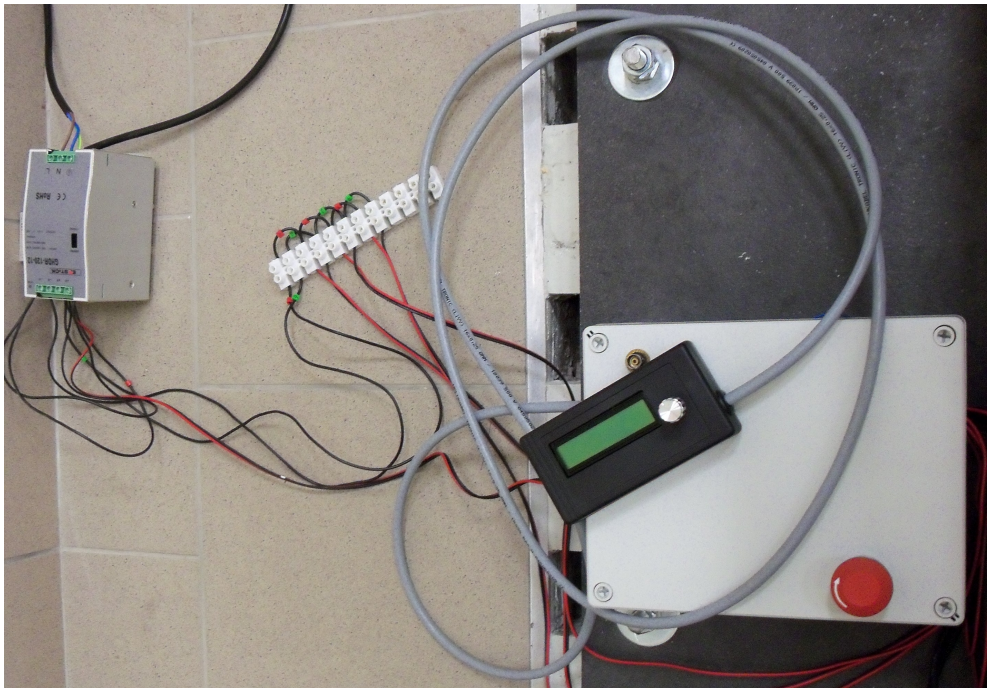

Fig. 4.3: Final circuit electronic - main box and operation panel

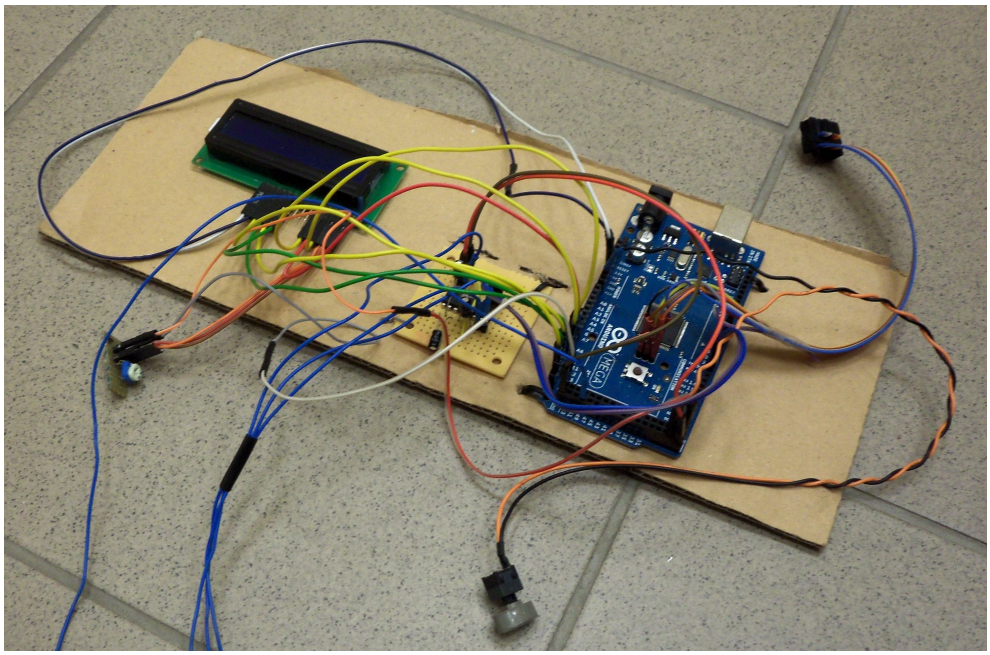

Fig. 4.4: Final circuit electronic - measurement and data transmission systems

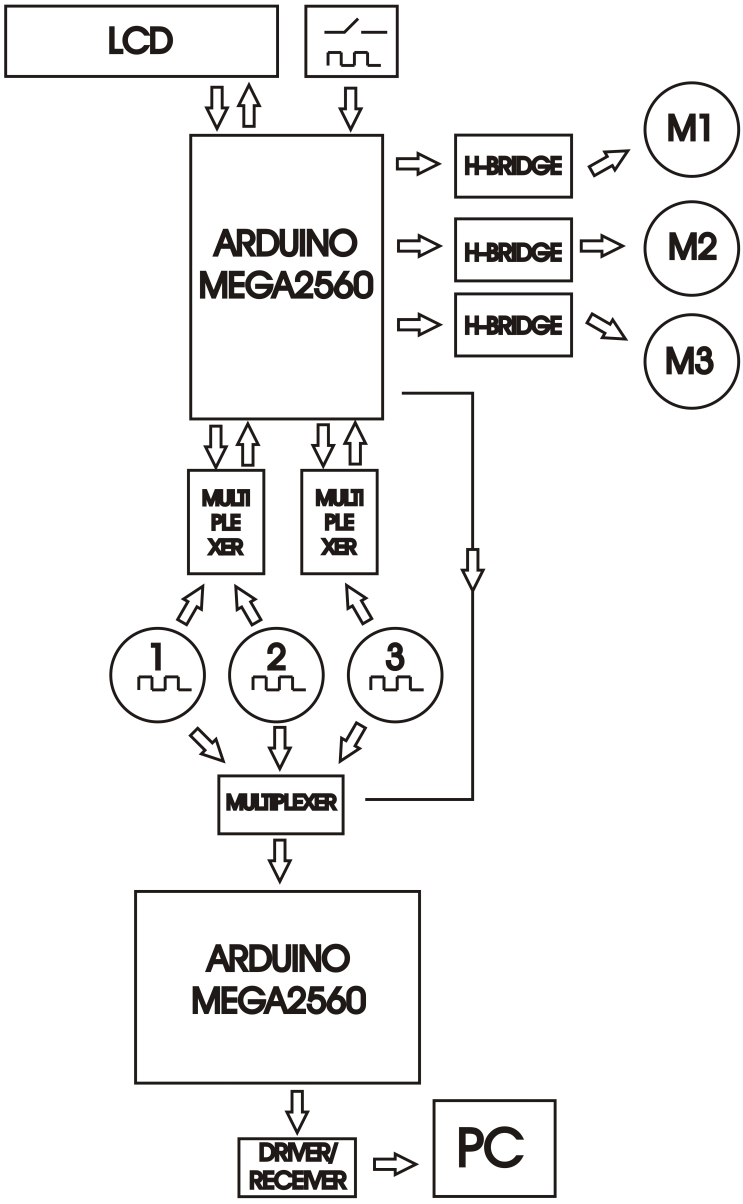

Fig. 4.5: Logical schematic of electronic circuit

4.4 Software

The system presented is based on AVR microprocessor programmed in C language which was developed on the basis of materials placed in in Tomasz Francuz book [13]. All functions are available from bidirectional list menu. According to the suggestion all structure of menu was placed in FLASH memory due to save place in SRAM memory. Relation between menu items is

declared in structures which are assigned to the menu elements. Navigation through menu is possible with mechanical encoder with includes the button used to select or abort functions. Menu structure is shown below:

- Motor settings
  - » Set Duty Cycle
    - * 2 Motors
      - · 1 Motor Speed
      - · 3 Motor Speed
      - · Both Motor speed
      - · Align the faster
      - · Align the slowest
    - * 3 Motors
      - · 1 Motor Speed
      - · 2 Motor Speed
      - · 3 Motor Speed
      - · All Motor speed
      - · Align the faster
      - · Align the slowest
  - » Set Act. Speed
    - * 1 Motor Speed
    - * 2 Motor Speed
    - * 3 Motor Speed
    - * All Motor speed
    - * Choose accuracy
      - · set accu. to 0,5
      - · set accu. to 1
    - * Execute
  - » Stop All
  - » Start All
- Measurements
  - » 2 Motors
  - » 3 Motors
- Authors

The menu that is presented above has two basic functionalities that are control and measure of motor speed. Their technical aspects are presented in subsections below. Reading signals from encoders gave possibility to improve control of motor speed. This means that user will be able to correct duty cycle in order to make all motor speed same. It is also possible to make that correction automatically using "Set Actual Speed" submenu. In automatic mode user can choose alignment accuracy. Another method of changing motor speed is setting duty cycle of PWM signal. In both modes and depending on the selected function, user can adjust the speed of single-engine, two or three engines at the same time. Another function is possibility to check motor speed by dedicated submenu - Measurements. .

4.5 PWM signal

PWM signal is integrated with timer/counter microprocessor feature. According to datasheet [6] timer has different modes of operation in case of ATmega2560 there are 12. Timer can count from bottom to top value or in the oposite direction. Bottom value is 0 for all modes but top can be chosen from standard varibles or manually setted in specified registers. Fast PWM, 8-bit was chosen because it is accurate enough for the aimed task. This mode is different from other modes by single-slope operation which means it always starts counting from bottom value. This feature make it suitable for power regulation. PWM signal can be characterized by three values: resolution, frequency and duty cycle. In presented system resolution of fast PWM is fixed to 8-bit. The PWM frequency can be calculated by the following equation:

$$f_{OCnxPWM} = \frac{f_{clkI/O}}{N * (1 + TOP)} \tag{4.1}$$

Frequency of PWM signal has been set as $f_{OCnxPWM} = 61,04\ Hz$.

4.6 Reading signal frequency

Reading signal from high resolution rotation encoders is complicated because signal changes rapidly. The main challenge with reading such external and high speed signals is to assign enough processor capacity for handling the incoming events. In many articles the problem is solved by using two timers/counters. In this case first timer measure the time interval and the second one is a counter. This approach is not effective because it involves two timers. Moreover accuracy of measurement demands sofficient number of cycles, impulses which can become source of problems in case of low frequency of the signal. As it was mentioned before the laboratory station involves three slowly rotating pendulums. Slowly in this context means speed range: 200 - 700 rpm. As a

result signal hes a wide range of frequency. Other solution is based on the ICP - input capture unit which is an integral part of the 16-bit Timer/Counter. This way uses only one timer which instantly leads to the conclusion about the advantages of this approach. ICP feature allows to capture external events and give them a time-stamp. That value can be used to indicate time of occurrence of the event. That creates the possibility to catch external signal and place actions in time. Signal can be applied via the ICPn pin but in case of the Timer/Counter1 it is possible to use Analog Comparator unit. The time-stamps are useful for calculation frequency and duty-cycle for example. The most important property of the ICP is setting Input Capture flag in the same system clock as the timer value is copied into output register. This flag can be cleared automatically or by software [6].

4.7 USART Interface

According to the information presented in Tomasz Francuz book [13] these interface is still commonly used in the technique. Interfaces of this type demands crossing Rx i Tx signals, which allows the connection of two devices only. In standard connection form transmission is asynchronous. The most important fact is different electric signals levels between TTL and RS232 standard. In consequence it is necessary to use transreceiver circuit. One of commonly used is MAX232 which was used in presented application [14].

Setting RS232 transmission, it is necessary to set communication speed which is processor speed divided by value of Baud Rate Register. It is possible to use library functions to make the settings right, what was done in program. Another issue is to set the frame format. In presented system frame format is as follows: start bit, eight data bits, two stop bits.

Data transfer is able due to save data in two-step buffer - UDR register. Transmission can be triggered on the basis of the UDRE or the TXC bit state. They respectively represent emptied buffer and complete transmission [6]. From computer - receiver site data are govered with usage of Bray Terminal 1.9b.

Chapter 5

First model's synchronizations

Every four synchronizations, by first model, were obtained. In Figures 5.1 and 5.2 can be observed completely and phase synchronization of two terminal pendulums. The middle one is caged. Whereas in Figures 5.3 and 5.4 can be observed completely and phase synchronization of three pendulums.

Nevertheless, as it is said in chapter 3. this model was not sufficient enough.

Fig. 5.1: Two pendulums' completely synchronization

Fig. 5.2: Two pendulums' synchronization at 180° intervals

Fig. 5.3: Three pendulums' completely synchronization

Fig. 5.4: Three pendulums' synchronization at 120° intervals

Chapter 6

Measurements and elaborated results

To easier obtain synchronizations of pendulums at actual model, first simulations by mathematic model were realized, to get approximate angular velocities $\dot{\varphi}_1$, $\dot{\varphi}_2$, $\dot{\varphi}_3$ of pendulums. Knowledge of angular velocities lets to narrow an area of searching.

To check if pendulums are synchronized stroboscopic lamp were used. Every time getting synchronization it was necessary to check if frequency of flash is appropriate, reducing it by half. Also during synchronizations, the system changes emitted sound.

Every measurements were realized using safety cage.

6.1 Two pendulums

6.1.1 Two pendulums' completely synchronization

During searching synchronizations of two pendulums two terminal pendulums were used. A middle one is left on the beam, but caged.

In Figure 6.1 is shown the actual model's completely synchronization. In Figure 6.2 are shown time histories of pendulum's velocity, during one period, from actual model and numerical simulation.

Fig. 6.1: Actual model's two pendulums' completely synchronization

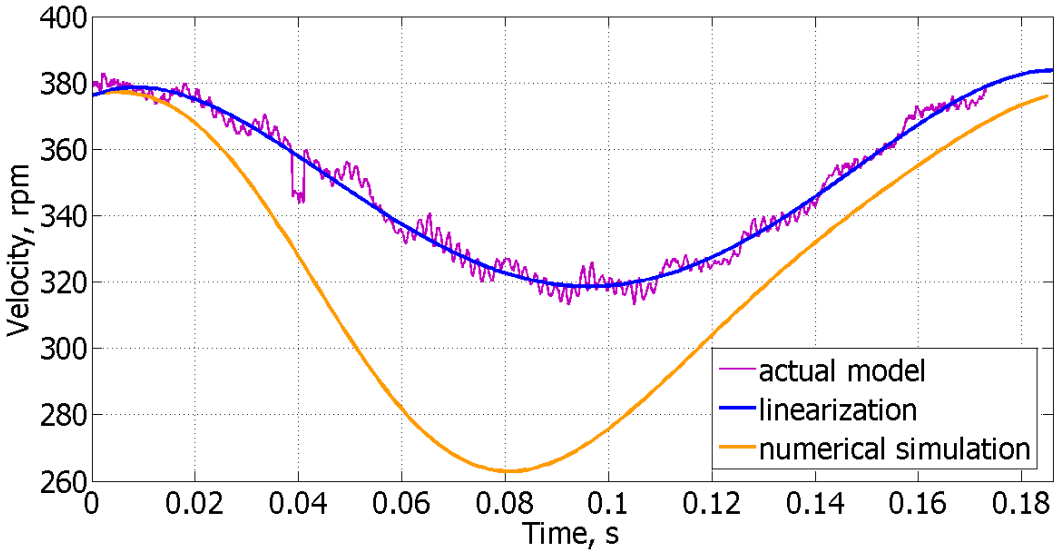

Fig. 6.2: Pendulum speed during one rotation - two pendulums' completely synchronization

6.1.2 Two pendulums synchronization at 180° intervals

In Figure 6.3 is shown actual model's synchronization at 180° intervals. In Figure 6.4 are shown time histories of pendulum's velocity, during one period, from actual model and numerical simulation.

Fig. 6.3: Actual model's two pendulums' synchronization at 180° intervals

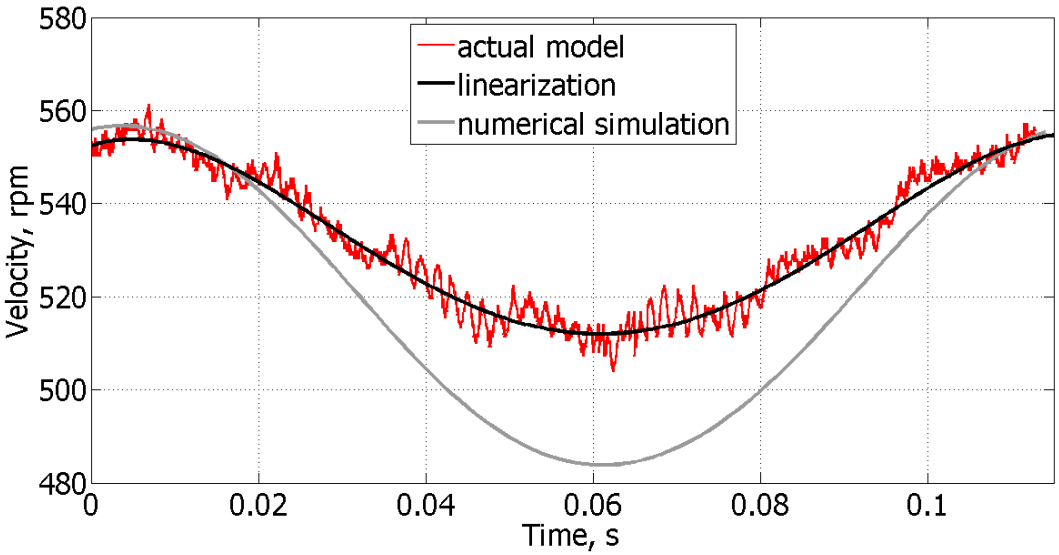

Fig. 6.4: Pendulum speed during one rotation - two pendulums' synchronization at 180° intervals

6.2 Three pendulums

6.2.1 Three pendulums' completely synchronization

In Figure 6.5 is shown actual model's completely synchronization. In Figure 6.6 are shown time histories of pendulum's velocity, during one period, from actual model and numerical simulation.

Fig. 6.5: Actual model's three pendulums' completely synchronization

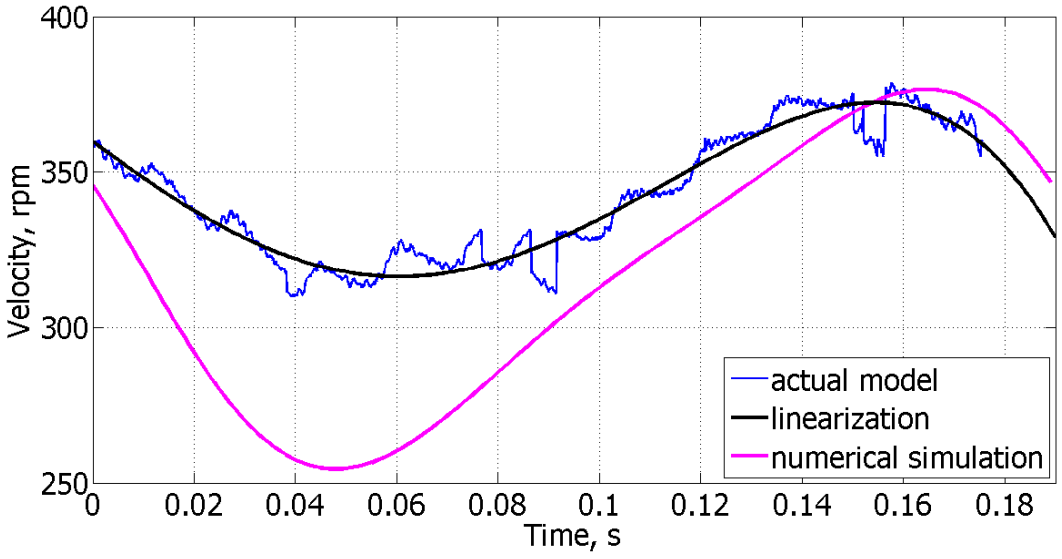

Fig. 6.6: Pendulum speed during one rotation - three pendulums' completely synchronization

6.2.2 Three pendulums synchronization at 120° intervals

In Figure 6.7 is shown actual model's synchronization at 120° intervals. In Figure 6.8 are shown time histories of pendulum's velocity, during one period, from actual model and numerical simulation.

Fig. 6.7: Actual model's three pendulums' synchronization at 120° intervals

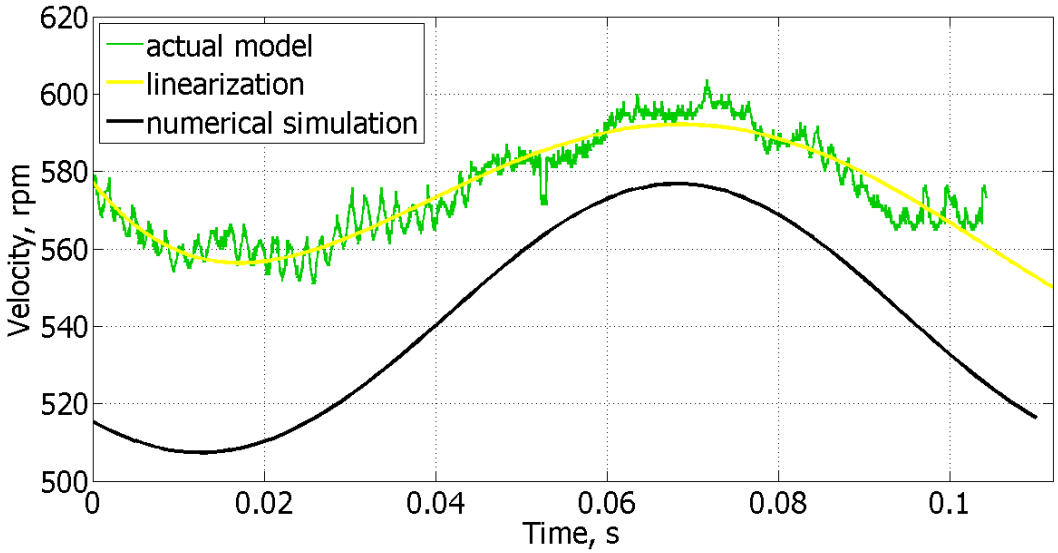

Fig. 6.8: Pendulum speed during one period - three pendulums' synchronization at 120° intervals

6.3 Oscillation periods

In Table 6.1 is shown oscillation periods,during synchronizations, of pendulums and beam measured by actual and numerical model.

Oscillation periods	**pendulum**		**beam**	
	actual	numerical	actual	numerical
2 complete	173	185	180	185
2 at 180 intervals	113	114	121	57
3 complete	176	189	182	188
3 at 120 intervals	104	110	111	36

Tab. 6.1: Oscillation periods in ms

Chapter 7

Conclusions

Change geometry of the laboratory station by reducing amount of freedom degrees, gave in consequence possibility to compare actual model and simulation results. It means that every motor have the same referring plane. In the end, presented system has four degree of freedom. Three rotating degree of freedom, one for every each pendulum and only one additional degree of freedom connected with beam movement.

Every synchronizations are obtained in both, simulation and actual model. Very small differences between actual and numerical results follows from accuracy of the systems. In numerical simulations the model is ideal with no external forces but gravity. While actual model is not perfect. The most problematic elements are hinges which have large clearances. In future work usage of professional bearings and replace the wooden beam by metal truss are planed.

To obtain synchronization, more important are velocities of pendulums, than initial conditions. Every pendulums' velocity has to be very similar to others. Small difference between velocities cases no synchronization. Complete synchronization is easier to obtain than interval. During interval synchronization, stabilization period amounts over 30s, whereas, during complete synchronization, the system stabilizes practically immediately. It means that, interval synchronization is more fine than complete, what was confirmed by actual and numerical models.

Comparing actual and numerical model in case of completely synchronization, disparities of oscillation periods of the beam and the pendulums, are considerable. Nevertheless, in both systems, oscillation period of the beam practically coincides oscillation periods of pendulums. Much better results are during interval synchronization. Oscillation periods of pendulums, in both, actual and numerical model, differ from each other of the order of 5% . In

numerical model the beam practically does not oscillate, while in actual model it does a little.

To sum up, the numerical model sufficiently replicates the actual model on present stage of researches. Future work will improve actual model and select new parameters for numerical model to reach better accuracy which needs some small improvements.

Bibliography

[1] Awrejcewicz J.: Mechanika techniczna. Wydawnictwo Naukowo-Techniczne, Warszawa 2007.

[2] Czolczyński K., Perlikowski P., Stefański A., Kapitaniak T.: Synchronization of pendula rotating in different directions. Łódź 20xx

[3] Kapitaniak M., Czolczyński K., Perlikowski P., Stefański A., Kapitaniak T.: Synchronization of clocks. Physics Reports 517, 2012

[4] Czolczyński K., Perlikowski P., Stefański A., Kapitaniak T.: Synchronization of slowly rotating pendulums. Łódź 20xx

[5] Kapitaniak T.: Wstęp do teorii drgań. Łódź 2005

[6] Technical datasheet of Atmega 2560 8-bit Atmel Microcontroller. Atmel 2012

[7] Technical datasheet VNH5019A-E - H-bridge motor driver. STMicroelectronics 2010

[8] Technical datasheet of Atmega 328p 8-bit Atmel Microcontroller. Atmel 2012

[9] Technical datasheet of 7805 - positive-voltage regulator. Texas Instruments 1976, revised 2003

[10] Pololu product information of VNH5019 Motor Driver Carrier: http://www.pololu.com/catalog/product/1451

[11] Technical datasheet of MOK50 encoder. Wobit 2002

[12] Technical datasheet of 4051 Single 8-Channel Analog Multiplexer/Demultiplexer. National Semiconductors 1989

[13] Tomasz Francuz. Język C dla mikrokontrolerów AVR. Helion, Gliwice 2011. ISBN 978-83-246-3064-6.

[14] Technical datasheet of MAX232 dual driver/receiver. Texas Instruments 1989, revised 2004